Determination of the cosmic-ray-induced neutron flux and ambient dose equivalent at flight altitude

Determination of the cosmic-ray-induced neutron flux and ambient dose equivalent at flight altitude

M T Pazianotto[1], M A Cortés-Giraldo[2], C A Federico[3], O L Gonçalez[3], J M Quesada[2], B V Carlson[1]

[1]Aeronautics Technological Institute, Physics Department, São José dos Campos, Brazil
[2]University of Sevilla, Atomic, Molecular and Nuclear Physics Department, Sevilla, Spain
[3]Institute for Advanced Studies, Applied Physics Department, São José dos Campos, Brazil

E-mail: mpazianotto@gmail.com

Abstract. There is interest in modeling the atmosphere in the South Atlantic Magnetic Anomaly in order to obtain information about the cosmic-ray induced neutron spectrum and angular distribution as functions of altitude. In this work we use the Monte Carlo codes MCNPX and Geant4 to determine the cosmic-ray-induced neutron flux in the atmosphere produced by the cosmic ray protons incident on the top of the atmosphere and to estimate the ambient dose equivalent rate as function of altitude. The results present a reasonable conformity to other codes (QARM and EXPACS) based on other parameterizations.

1. Introduction

Great efforts are being made to understand the accumulated neutron dose at flight altitude in the South Atlantic Magnetic Anomaly (SAMA) [1,2], because a large part of Brazil, and therefore South America, are subject to this Anomaly. Figure 1 shows that the SAMA at 12 km altitude is located with its center point above Brazil, near Foz do Iguaçú city.

Among the many particles produced by interactions between primary cosmic rays and atmospheric atoms, neutrons are the most important component to consider in order to assess the dose deposition in the crew members of an aircraft, as well as in electronic equipment, such as on-board computers [3]. Thus, there is great interest in modeling the atmosphere and simulating the cosmic-ray induced neutron spectrum at flight altitude to develop further applications for the study of their effects on microelectronic devices [4] and carry out dosimetry studies aboard aircrafts. The purpose of this work is to determine the cosmic-ray-induced neutron (CRINS) flux in the atmosphere produced by protons using the codes MCNPX [5] and Geant4 [6] and then to estimate the ambient dose equivalent rate (ADER) through the atmosphere. In this work, we are evaluating the Geant4 by comparing it with MCNPX and other codes in order to search possible effects of the Earth's magnetic field on the neutron flux as well on the ADER in flight altitude. The magnetic field can be easily included in Geant4, but not in MCNPX v2.5 and in the other codes used in this comparison.

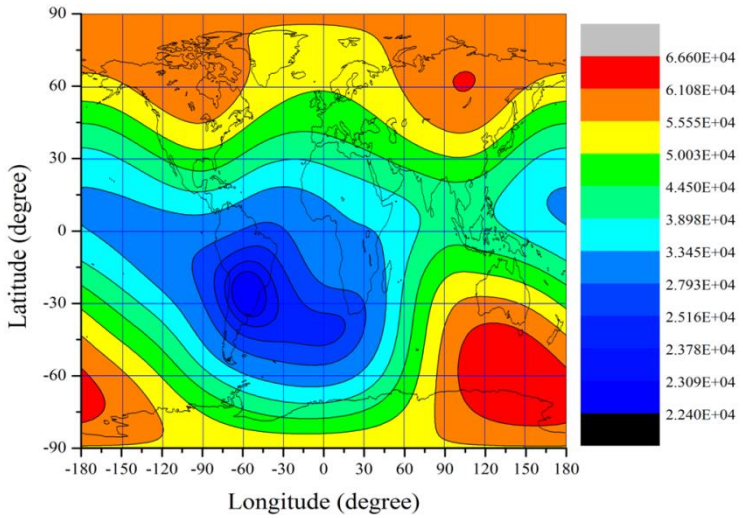

Figure 1. Earth's magnetic field map at 12 km altitude, taken from [7].

2. Methodology

2.1. Computational procedure

Figure 2 shows the geometry of the atmosphere used in the simulations. The atmosphere was modeled as a cylinder of 50 km height and 25 km radius. For the sake of reproducing the variable density of the atmosphere at different altitudes, the cylinder was divided into layers of 2.5 km thickness below 12.5 km altitude, whereas 5 km layers where used above this altitude level. The air density and composition of each layer was set according to the International Standard Atmosphere [8]; the air humidity was also modeled below 12.5 km altitude [9].

In order to reproduce an infinite medium, we used fully reflective sidewalls of the cylinder for all the particles that impinge on them. We used a primary cosmic ray flux composed only of protons at the top of the cylinder. The primary proton spectrum was obtained from QARM [10] at the geographical coordinates -23.04 S -45.15 W and at the date June 06, 2009.

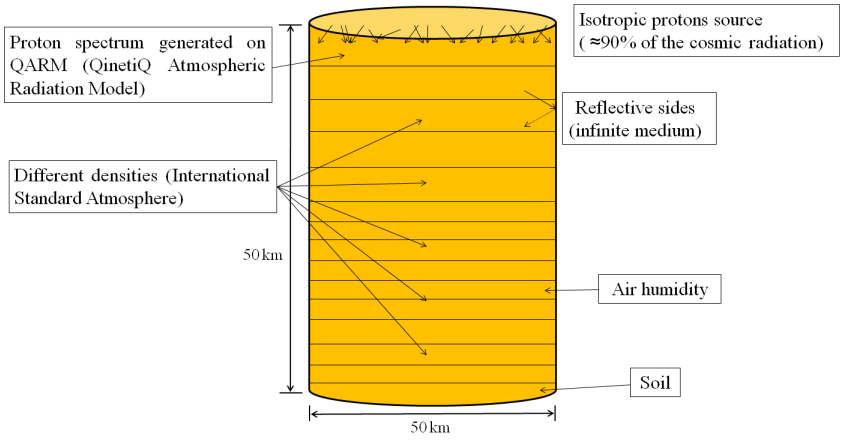

Figure 2. Schematic figure of the atmosphere modeling for cosmic ray propagation.

2.2. MCNPX physics models

In the simulations with MCNPX v2.5 the ENDF/VI nuclear data library was used for all materials. We considered the scattering matrices S(α,β) [5, 11] to correct the hydrogen cross section in water, which is important for neutron transport at low energies. Nuclear data libraries were used for neutron energies under 20 MeV. Physical models were used above this energy range according to the following parameterizations:

- Neutron and proton interaction only by elastic scattering;
- Bertini intranuclear cascade for nucleons, followed by pre-equilibrium;
- Coulomb barrier for incident charged particles;

2.3. *Geant4 physics models*

The simulations were carried out with the version 9.6.3 and 9.6.2 of the GEANT4 toolkit. For incident energies above 10 GeV, the hadronic interactions have been modeled with the Quark-gluon String Model (QGS). At lower energies, which are the most relevant in the present work, we used either the same hadronic modeling (Bertini Model) as MCNPX in the intranuclear cascade phase, followed by preequilibrium (physics list QGSP_BERT_HP), or the Binary Cascade, followed by the Exciton Pre-equilibrium model and final equilibrium de-excitation with a variety of models (Weisskopf-Ewing evaporation of nucleons and light clusters, photon emission, fission, Fermi break-up and statistical multifragmentation) as final stages (physics list QGSP_BIC_HP). For the transport of neutrons below 20 MeV, the High Precision (HP) model with G4NDL4.0 data was used.

3. Results

3.1. Comparison between MCNPX and Geant4

Figure 3 shows the integral neutron flux as a function of altitude calculated with MCNPX and Geant4. The simulations were performed using an enough events so that the statistical errors are significantly smaller than the values of the simulated data. The agreement between the MCNPX and the Geant4 simulations with the QGSP_BERT_HP physics list is certainly due the fact that the Bertini intranuclear cascade model is used in both cases. However, the agreement with the calculations done with the QGSP_BIC_HP physics list is observed only at 5 km altitude. For altitudes higher than 5 km, the QGSP_BIC_HP simulations predict a lower neutron counting rate, whereas at lower altitudes the situation is the opposite, i.e., they produce a higher neutron counting compared to those of MCNPX and the QGSP_BERT_HP Geant4 physics list.

As a preliminary analysis, the origin of this divergence could be traced back to the different neutron multiplicities of each model. At present, we are evaluating the primary proton integral flux as a function of altitude in an attempt to establish the connection between the number of neutrons produced and the protons absorbed throughout the atmosphere, which should provide us with a deeper understanding of this phenomenology.

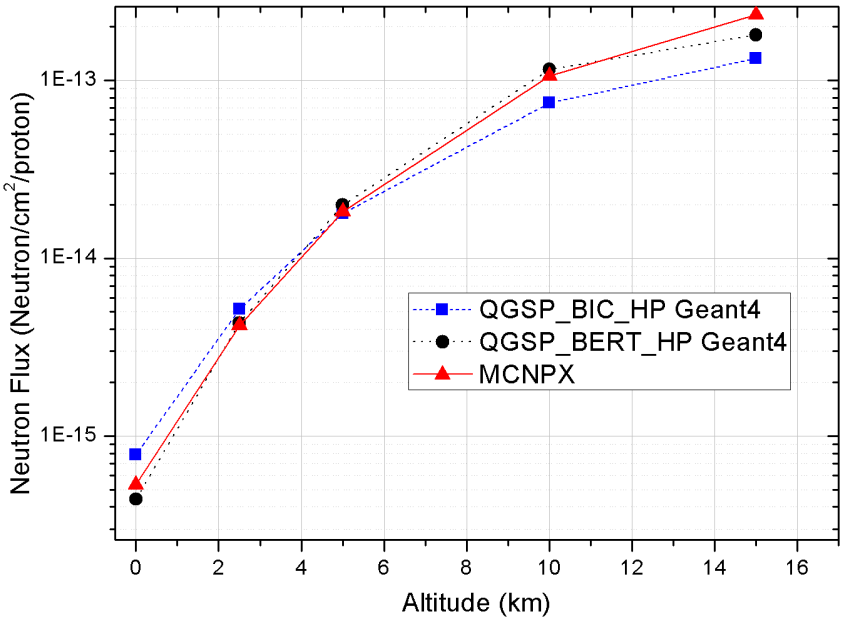

Figure 3. Integral neutron flux calculated with MCNPX and Geant4 with QGSP_BIC_HP and QGSP_BERT_HP physics lists.

Figure 4 shows the cosmic-ray induced neutron spectrum normalized per primary proton at 1 m (i.e., ground level) and 15 km altitude as simulated by MCNPX and Geant4 with the BIC and Bertini models. We observe a higher neutron production by spallation reactions at ground level with the Binary Cascade model of Geant4 than with the Bertini model. However, we have just the opposite at 15 km altitude.

In the thermal region at 1 m altitude, the neutron flux simulated with Geant4 is lower than the one simulated with MCNPX. This fact could be also explained due to the different neutron multiplicity of each model as previously mentioned.

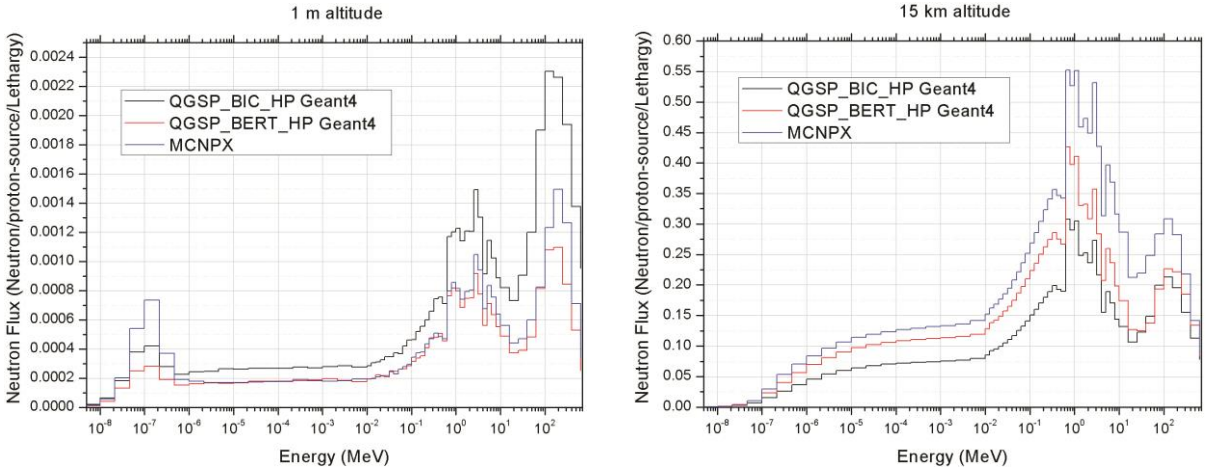

Figure 4. Neutron spectrum calculated at 1 m and 15 km altitude with MCNPX and Geant4 with QGSP_BIC_HP and QGSP_BERT_HP physics lists.

Figure 5 compares the neutron flux calculated with MCNPX, GEANT4 (using QGSP_BIC_HP) and EXPACS [12] with the experimental data from Federico et al [2] measured at 1 m altitude in São José dos Campos and other experimental results taken from the Goldhagen et al [13]. The results were normalized to 1 neutron/cm^2 integral flux in order to analyze only the energy dependence of the neutron spectra. At the thermal peak there is a wide dispersion of results, where the experimental measurement of Federico et al. [2] shows the largest amplitude and the Geant4 simulation has the smallest amplitudes. However, the results of MCNPX, EXPACS and Goldhagen somewhat agree among themselves. As well as the previous results (Figure 4), the energy dependence of the MCNPX and Geant4 simulations reproduce well the shape of the spectrum between the thermal and evaporation peaks, and these, in turn, reproduces well the experimental results of Goldhagen et al [13], but overestimate the experimental results of Federico et al [2]. However, the spallation region is clearly overestimated in the MCNPX and Geant4 calculations. The divergence between these results could be explained by the concentration of water used in the simulations, since the relative height of the peaks depends strongly on this [14]. A deeper study of this dependence is being carried out.

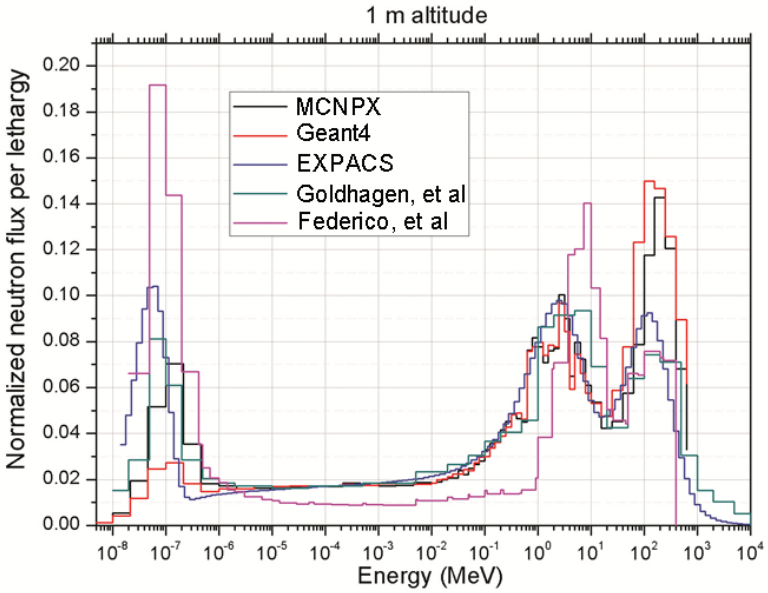

Figure 5. Energy dependence of the neutron flux at 1 m altitude calculated with EXPACS, MCNPX, GEANT4 and measured experimentally [3,12].

3.2. Ambient dose equivalent rate as a function of altitude

Figure 6 shows a comparison of the integral neutron flux per incident proton as a function of altitude between our Monte Carlo simulations with MCNPX and Geant4, and QARM code. The results present a reasonable conformity throughout for altitudes that ranges from 2.5 km to 15 km, but for ground level there is a divergence between our Monte Carlo simulations and QARM that could be explained due to the soil composition used on QARM code, information which could not be retrieved.

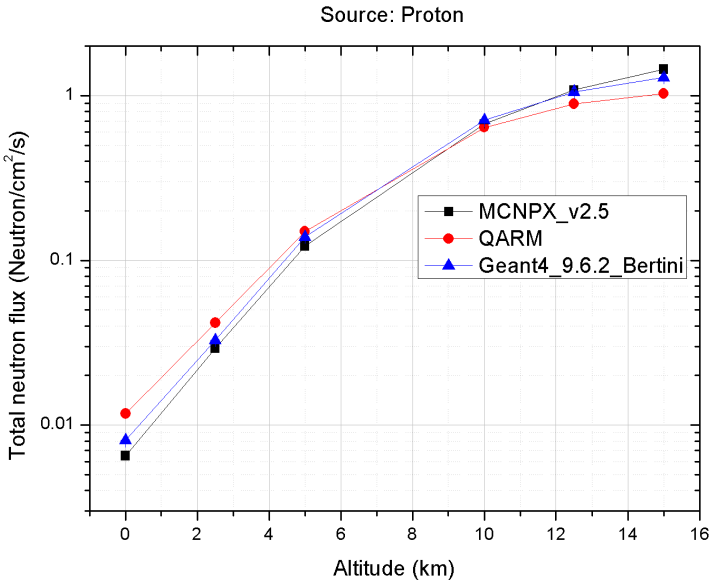

Figure 6. Absolute neutron flux as function of altitude determined by MCNPX, Geant4 and QARM.

Figure 7 compares the ambient dose equivalent rate obtained with MCNPX, GEANT4 and QARM. In order to determine the ambient dose equivalent rate, we multiplied the CRINS spectra by the integral proton flux at the top the atmosphere to obtain the CRIN in absolute value and then multiplied these spectra by a conversion factor that can be found in the ICRP74 data [15].

From this figure it can be seen that there is a remarkable agreement at 10 km altitude between the three codes. QARM gives the highest equivalent ambient dose values at altitudes lower than 10 km, whereas at higher altitudes the values predicted with both Monte Carlo codes are higher than those of QARM; nevertheless, the agreement between the calculations is quite reasonable.

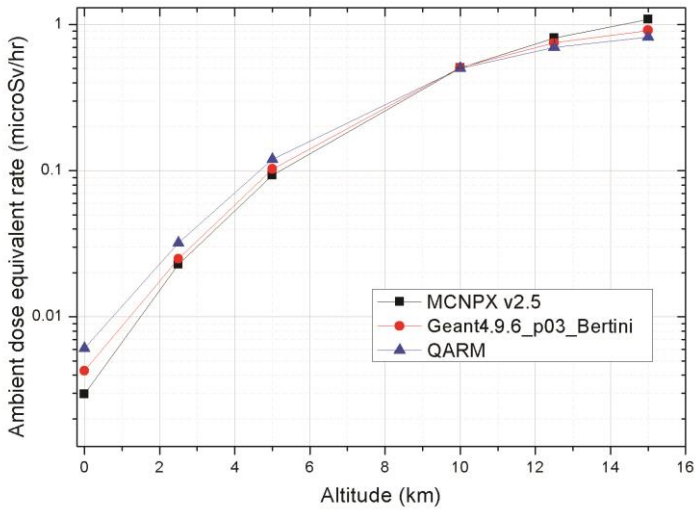

Figure 7. Ambient dose equivalent rate as function of altitudes.

As a first order approximation, we have initiated a study of the influence of Earth's magnetic field on the ambient dose equivalent rate. To do this, we have used the Geant4 code together with terrestrial

magnetic field data from [16] at the geographical coordinates 23.04 S 45.15 W on the date June 06, 2010, when its horizontal intensity was 18,528.8 nT. Figure 8 shows the comparison of the ADER considering the Earth's magnetic field and excluding it. The magnetic field does not change the ADER for altitudes between 1 m up to 45 km, where the air density is very low compared to the ground level.

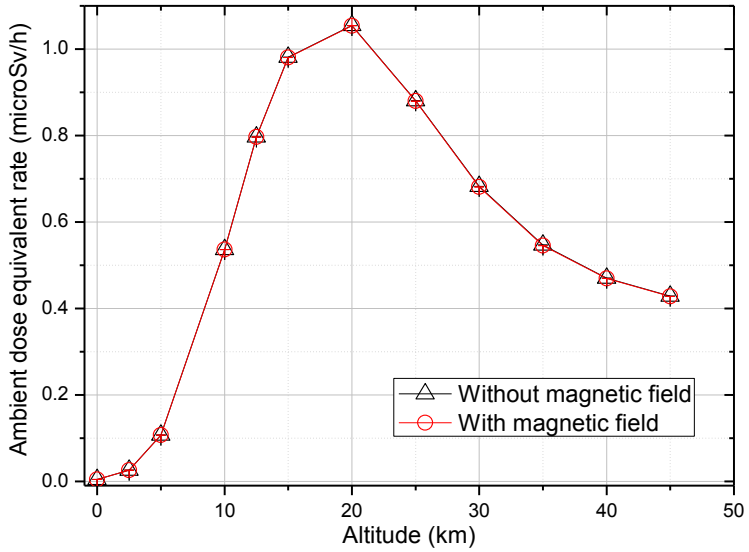

Figure 8. Ambient dose rate versus altitude calculated with GEANT4. The Earth's magnetic field was turned on and off for comparison.

4. Conclusions

The comparison between our Monte Carlo simulations with MCNPX (version 2.5) and Geant4 (version 9.6.2 and 9.6.3) and the calculations obtained with the codes QARM and EXPACS presents good general agreement, although a difference exists at 1 m altitude that could be explained by soil composition. For future work, a detailed analysis of the soil composition influence will be necessary.

As a first order approximation, the Earth's Magnetic field does not change the ambient equivalent dose rate for altitudes up to 45 km. Ongoing studies with the Geant4 toolkit and analytical calculations are being performed to quantify the influence of the Earth's magnetic field on the primary and secondary particles throughout the atmosphere and on the particle angular distributions as a function of altitude.

References

[1] Freden S C and Paulika G A 1964 Trapped protons at low altitudes in the South Atlantic magnetic anomaly *Jour. of Geophysical Research* vol 69 pp 1259-1269.
[2] Federico C A *et al* 2010 Neutron spectra measurements in south Atlantic anomaly *region Rad. Measurements* vol. 45 pp 1526-1528
[3] Prado A C M *et al* 2013 Effects of cosmic radiation on devices and embedded systems in aircrafts *2013 International Nuclear Atlantic Conference*
[4] Pereira Junior E C F *et al* 2014 The effects of total ionizing dose on the neutron SEU cross section of a 130 nm 4 Mb SRAM memory *Proc 15th Latin American Test Workshop*
[5] Pelowitz D 2005 MCNPX User's Manual Version 2.5.0 *Los Alamos National Laboratory report LA-CP-05-0369*
[6] Agostinelli S *et al* 2003 GEANT4 – a simulation toolkit *Nucl Instr Meth Phys Res A* vol 506(3) pp 250-303
[7] Space Environment Iformation System. Available at: www.spenvis.oma.be.
[8] International Organization for Standardization 1975 Standard Atmosphere ISO 2533:1975 1975
[9] Salby M L, Pielke R A, Dmowska R 1996 Fundamentals of Atmospheric Physics *International Geophysics* vol 61.
[10] Lei F, Clucas S, Dyer C, Truscott P 2004 An atmospheric radiation model based on response matrices generated by detailed Monte Carlo Simulations of cosmic ray interactions *IEEE Transactions on Nuclear Science* vol 51
[11] Mattes M and Keinert J Thermal Neutron Scattering Data for the Moderator Materials H2O, D2O and ZrHx in ENDF-6 Format and as ACE Library for MCNP(X) *Codes IAEA report INDC(NDS)-0470*
[12] Sato T EXPACS User's Manual *Japan Atomic Energy Agency*
[13] Goldhagen P *et al* 2002 Nucl Measurement of the energy spectrum of cosmic-ray induced neutrons aboard an ER-2 high-altitude airplane *Nuclear Instruments and Methods in Physics Research A* vol 476 2002
[14] Nakamura T *et al* 2005 Sequential measurements of cosmic-ray neutron spectrum and dose rate at sea level in Sendai *Japan. J. Nucl. Sci. Technol.* vol 42
[15] ICRP 1996 Conversion Coefficients for use in Radiological Protection against External Radiation ICRP Publication 74 Ann. ICRP 26 (3-4)
[16] Earth's Magnetic Field Calculators. Available at: https://www.ngdc.noaa.gov/geomag/magfield.shtml